Proceedings of the 28th IEEE
EMBS Annual International Conference
New York City, USA, Aug 30-Sept 3, 2006

Iridium sputtered at varying pressures and target-substrate-distances evaluated for use as stimulation electrode material

Boerge Wessling, André van Ooyen, Wilfried Mokwa, and Uwe Schnakenberg

Abstract—**Iridium was sputtered as the top layer of stimulation electrodes. The coatings were varied in their morphology by adjusting the total deposition pressure and the working distance (WD) of target and substrate. It is shown that the resulting different kinds of morphologies have a strong influence on stimulation characteristics. The combination of high working gas pressure and small WD as well as the combination of medium working gas pressure and larger WD yield the best characteristics on macro-sized test electrodes.**

I. Introduction

The neural stimulation and recording electrodes integrated into functional medical implants need to feature high charge injection capacities and low impedance characteristics. Especially in small implants based on micro system technologies, the stimulation sites need to exhibit low interface losses and high resolution. An example for the high demands on electrode stimulation performance and power consumption is the wireless EPI-RET implant aiming to restore a sense of vision in people suffering from blindness due to retinitis pigmentosa [1].

In order to evoke an action potential in neuronal cells such as the retinal ganglion cells, certain amounts of charge need to be delivered to the tissue [2]. The amount of reversibly transferred charge is determined by size and charge per area of the electrode, where the latter depends on the stimulation material. A higher charge delivery capacity allows for a smaller electrode design, which increases the stimulation resolution.

Apart from other biocompatible materials such as platinum [3], titanium or titanium nitride [4], promising candidates for functional coatings of stimulation electrodes are iridium and iridium oxide (IrOx). They can be deposited by several methods, for example electrochemically from solution [5, 6], by electrochemical activation of pure iridium [7, 8] or by reactive laser ablation [9]. A further approach is (reactive) sputtering, where the performance of IrOx electrodes strongly depends on the deposition parameters. A number of investigations regarding IrOx process parameters have already been made. For instance, the oxygen flow to the plasma chamber during sputtering [10, 11] and the film thickness [12] were varied and linked to stimulation behavior. Improved stimulation characteristics were related to altered microstructures, mainly attributing enhanced charge injection to a higher specific surface.

Thornton found that the microstructure of different coatings such as Cu, Fe or Ni can be varied between three different zones by adjusting total sputter pressure and temperature [13]. Taking his structure zone model as a starting point, several authors expanded the principle to further materials and sputter parameters such as sputter angle [14], target-substrate working distance (WD) [15] and deposition rate [16]. Thornton's zone I microstructure is most suitable for electrode coatings. It is characterized by a columnar surface structure with voids, the surface is composed of hillocks. A zone I microstructure generally evolves from conditions of low adatom mobility and high shadowing effects. Shadowing effects occur if atoms impinge at an angle and not orthogonal to the substrate. This way, high points on the surface receive more flux than low points, and hillocks and valleys develop. Due to low mobility (no additional substrate heating, low incident atom energy), adatom diffusivity is limited and atom configurations scarcely reorganize, leaving the microstructure voided and rough [17].

Focusing on macro-sized electrodes, we describe the variation of shadowing effects and surface mobility by adjusting total sputtering pressure and WD of thin Ir films, explicitly excluding oxygen addition.

It is shown that this set of deposition parameters can be effectively used to change and adjust Ir deposit morphology and electrode performance.

II. Experimental

A Nordiko NS 2550 sputtering tool was employed to deposit Ir and IrOx thin films in Ar or Ar/O_2 plasmas. In order to enhance adhesion, a thin Ti layer was placed between SiO_2 substrate and electrode material. The film thicknesses were determined via lift-off process with a Tencor PA-10 profilometer. All films described here were deposited to Ir thicknesses around 300-350 nm. Prior to deposition, the sputtering chamber was evacuated to at least 4×10^{-6} mbar by means of a cryogenic pump. To determine the charge delivery characteristics of Ir films, cyclic voltammetry (CV) was performed in physiological saline solution (0.9% NaCl) using an Ag/AgCl reference and a Pt-

Manuscript received April 2, 2006. This work was supported by the German Research Foundation under Grant Graduate School GRK 1035 Biointerface and the German Federal Ministry of Education and Science under grant EPI-RET.

Author and co-authors are with the Institute of Materials in Electrical Engineering I, RWTH Aachen University, Germany. (phone: +49-241-80-27759; fax: +49-241-80-22392; e-mail: wessling@iwe1.rwth-aachen.de).

wire counter electrode. The Ir electrodes had surface areas of 0.503 cm^2. Their potential was cycled inside the water window of the system between about -1 V and +1.3 V, i.e. excluding H_2 and O_2 evolution, at a scan rate of 100 mV/s. In order to evoke higher electrochemical activity, Ir thin films were repeatedly cycled within the safe potential range.

Impedance measurements were performed in the same electrochemical cell. The disturbing sinusoidal signal had an amplitude of 10 mV, and its frequency was tuned from 1 MHz to 50 mHz.

In order to test electrode response to pulsed excitation, cathodic-first, charge balanced current pulses (2.5 ms duration, current amplitudes between 2.5 mA and 100 mA) were applied and the corresponding driving voltages were evaluated after correction for iR-drop including electrolyte.

III. Results and Discussion

Figures 1 a) and b) show CV and impedance data of samples deposited at 1 kW DC input power, a WD of 45 mm and varying total pressure of 1.6 x 10^{-2}, 9.3 x 10^{-2} and 1.7 x 10^{-1} mbar, each after 100 activation cycles.

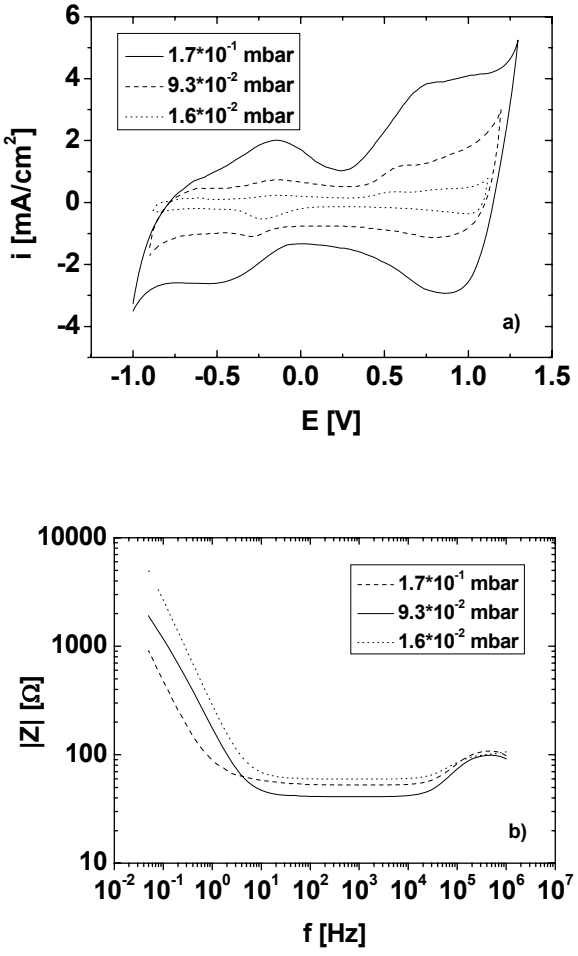

Fig. 1. a) CV data and b) Bode plots of three Ir samples deposited at different Ar pressures.

It becomes clear that a higher working gas pressure leads to electrochemically more active films. CV curves are more expanded and the charge delivery capacity Q_d, calculated as cathodic or anodic charge from the integral of the CV curve, increases with pressure as shown in Table 1. As curve fitting showed, diffusion control plays a lesser role in impedance behavior of activated samples. This means that at lower frequencies, the electrode impedance is dominated by the double layer capacitance. Under these premises, the capacitance C_{dl} can be calculated from $|Z|=(\omega C)^{-1}$ at a frequency $\omega=1s^{-1}$. The capacitances were extracted and are also displayed in Table 1.

TABLE 1.
COMPARISON OF CHARGE DELIVERY CAPACITY AND DOUBLE LAYER CAPACITANCE OF SAMPLES DEPOSITED AT 1 KW POWER, A WD OF 45 MM AND DIFFERENT WORKING GAS PRESSURES

p [mbar]	Q_d [mC/cm^2]	C_{dl} [mF]
1.6 x 10^{-2}	4	0.5
9.3 x 10^{-2}	18	1.2
1.7 x 10^{-1}	46	3.2

As the Ar pressure in the chamber is increased, the number of collisions an atom undergoes while traveling from target to substrate increases, because the mean free path varies with pressure p according to

$$\lambda_m = \frac{k_B T}{r_{sg} \pi p}, \quad (1)$$

where k_B is the Boltzmann constant, T the gas temperature and r_{sg} the interatomic separation of sputtered atom and working gas [18]. This means that the mean free path is almost sextupled going from low to medium pressures, and again almost doubled going to the highest pressure. As a result of frequent collisions, incident angles are widely spread and shadowing is promoted. Also, the particle energy decreases. This leads to less diffusion of the arriving atom, less resputtering of film atoms, and minimizes local heating, which again decreases mobility.

The differences in morphologies are illustrated by SEM graphs shown in Fig. 2. In both cases, columnar microstructures typical of zone I develop. Note, however, that voids are visible between the columns only in the top part of Fig. 2, which shows the sample deposited at highest pressures. The conditions of lower mobility also bring about a rougher surface compared to the rather smooth hillocks visible in the bottom part of Fig. 2.

Similar investigations were performed choosing an input power of 1 kW DC and a constant medium Ar pressure of 9.3 x 10^{-2} mbar. In this series of investigation, the WD was varied between 45, 62 and 78 mm.

Table 2 summarizes the extracted data. Also in this case, deposition parameters have a strong influence on Ir electrode characteristics.

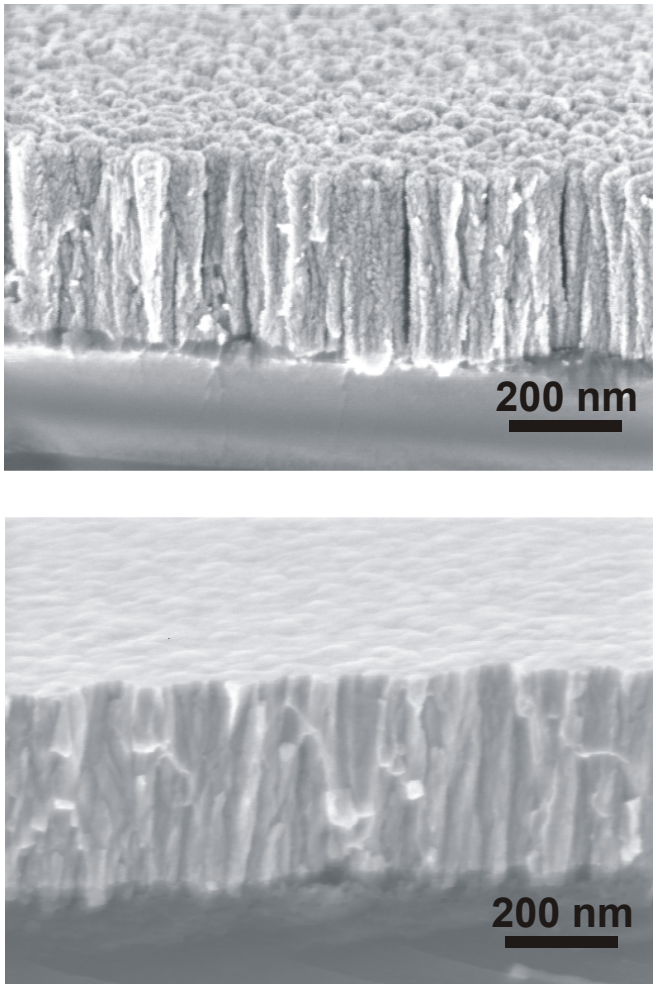

Fig. 2. SEM micrographs of samples deposited at pressures of 1.7 x 10^{-1} (top) and 1.6 x 10^{-1} mbar (bottom).

TABLE 2.
COMPARISON OF CHARGE DELIVERY CAPACITY AND DOUBLE LAYER CAPACITANCE OF SAMPLES DEPOSITED AT 1 KW POWER, A BACKGROUND PRESSURE OF 9.3 X 10^{-2} MBAR AND DIFFERENT WD

WD [mm]	Q_d [mC/cm^2]	C_{dl} [mF]
45	18	1.2
62	47	3.6
78	49	4.1

A too small WD, with the given parameters of pressure and input power, results in electrochemically less active samples. Energetic particle bombardment and local impact heating lead to higher diffusion activity. A rather smooth surface develops. It is shown in Fig. 3 (top), together with a surface graph of the sample deposited at a WD of 62 mm. Different from the sample deposited at lower WD, the film shown in the lower part of Fig. 3 is characterized by voids or grooves between the columns, which are also visible from the top.

Interestingly, from Table 2 one notices that an increase of WD from 62 to 78 mm does not seem to have any effect on electrode characteristics. Also when comparing micrographs, no difference between the samples is visible (the film deposited at a WD of 78 mm is not shown here). A possible explanation is that the number of in-flight collisions in the case of medium WD is large enough to reduce the particles' energies to those of the background gas atoms [19]. This means that an increase in WD and thus number of collisions does not have any further effect of reducing Ir particle energies.

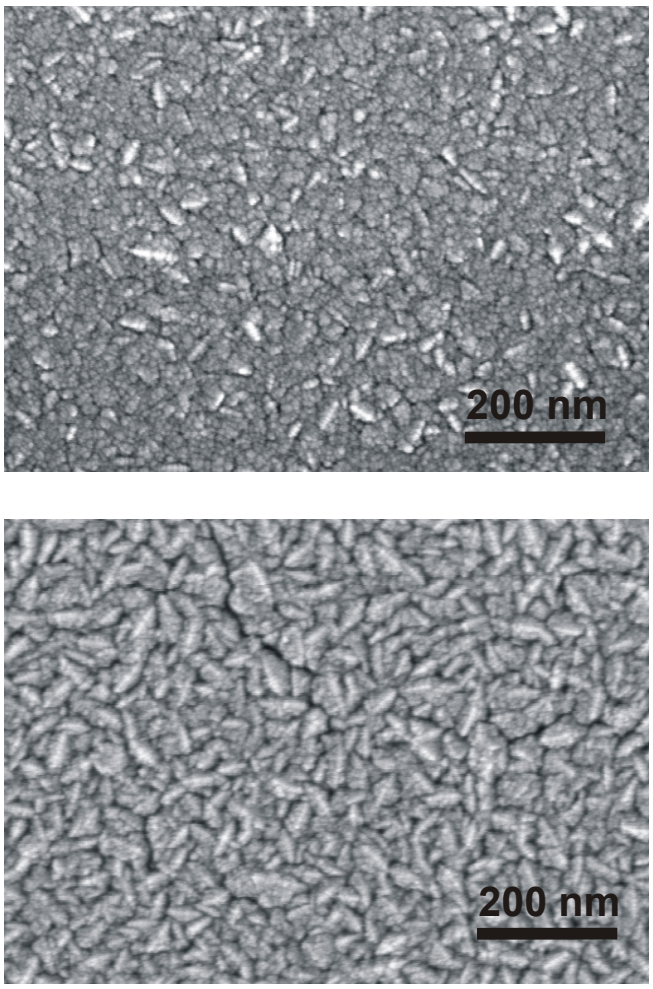

Fig. 3. SEM surface figures of samples deposited at WD of 45 (top) and 62 mm (bottom).

Note also that the combination of high working gas pressure and small WD (Table 1) as well as the combination of medium working gas pressure and larger WD (Table 2) lead to comparable results. This shows that it is possible to achieve similar conditions of low adatom mobility by choosing different parameter sets.

Biphasic current pulses of 2.5 ms duration were applied to the sample deposited at highest Ar pressure and smallest WD. The current amplitude was varied such that charge densities between 0.0125 and 0.25 mC/cm^2 were injected. The voltage required to drive the charge was corrected for iR-drop in the circuit and is shown versus the injected

charge density in Fig. 4. The values are of higher magnitude than those reported in [12]. However, it needs to be observed that the samples described here were thin and deposited without the addition of oxygen, which is known to significantly enhance charge injection capacities [10, 11].

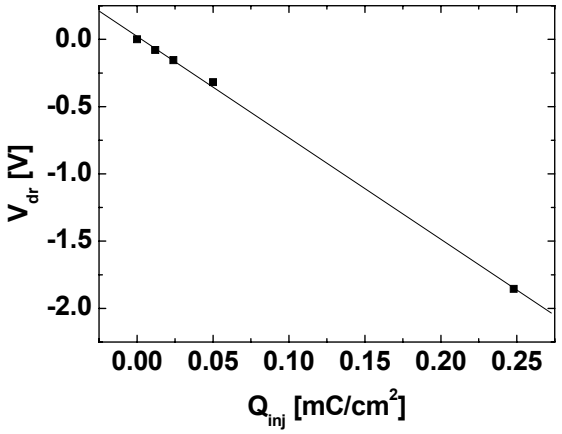

Fig. 4. Driving voltage versus pulse injected charge for the sample shown in the top of Fig. 2.

IV. CONCLUSION

It was shown that the sputter parameters total pressure and target-substrate distance can be used to tune the morphology of thin Ir films. The macro-electrode characteristics strongly depend on morphology, where a columnar and voided structure is most favorable for charge injection. The materials presented can serve as a basis for further electrode improvement, e.g. by way of oxygen supply during sputtering or film thickness increase.

REFERENCES

[1] W. Mokwa, "MEMS technologies for epiretinal stimulation of the retina," *Journal of Micromechanics and Microengeneering*, vol. 14, pp. 12-16, 2004.

[2] M. P. Maher, J. Pine, J. Wright, and Y. C. Tai, "The neurochip: a new multielectrode device for stimulating and recording from cultured neurons," *J Neurosci Methods*, vol. 87, pp. 45-56, 1999.

[3] T. L. Rose and L. S. Robblee, "Electrical-Stimulation with Pt Electrodes.8. Electrochemically Safe Charge Injection Limits with 0.2 Ms Pulses," *IEEE Transactions on Biomedical Engineering*, vol. 37, pp. 1118-1120, 1990.

[4] J. D. Weiland, D. J. Anderson, and M. S. Humayun, "In vitro electrical properties for iridium oxide versus titanium nitride stimulating electrodes," *IEEE Transactions on Biomedical Engineering*, vol. 49, pp. 1574-1579, 2002.

[5] S. C. Mailley, M. Hyland, P. Mailley, J. M. McLaughlin, and E. T. McAdams, "Electrochemical and structural characterizations of electrodeposited iridium oxide thin-film electrodes applied to neurostimulating electrical signal," *Materials Science & Engineering C-Biomimetic and Supramolecular Systems*, vol. 21, pp. 167-175, 2002.

[6] R. D. Meyer, S. E. Cogan, T. H. Nguyen, and R. D. Rauh, "Electrodeposited iridium oxide for neural stimulation and recording electrodes," *IEEE Transactions on Neural Systems and Rehabilitation Engineering*, vol. 9, pp. 2-11, 2001.

[7] A. Blau, C. Ziegler, M. Heyer, F. Endres, G. Schwitzgebel, T. Matthies, T. Stieglitz, J. U. Meyer, and W. Gopel, "Characterization and optimization of microelectrode arrays for in vivo nerve signal recording and stimulation," *Biosensors & Bioelectronics*, vol. 12, pp. 883-892, 1997.

[8] L. S. Robblee, J. L. Lefko, and S. B. Brummer, "Activated Ir - an Electrode Suitable for Reversible Charge Injection in Saline Solution," *Journal of the Electrochemical Society*, vol. 130, pp. 731-733, 1983.

[9] M. A. El Khakani and M. Chaker, "Reactive pulsed laser deposition of iridium oxide thin films," *Thin Solid Films*, vol. 335, pp. 6-12, 1998.

[10] E. Slavcheva, R. Vitushinsky, W. Mokwa, and U. Schnakenberg, "Sputtered iridium oxide films as charge injection material for functional electrostimulation," *Journal of the Electrochemical Society*, vol. 151, pp. E226-E237, 2004.

[11] B. Wessling, W. Mokwa, and U. Schnakenberg, "RF-sputtering of iridium oxide to be used as stimulation material in functional medical implants," *Journal of Micromechanics and Microengineering*, vol. 16, pp. S142-S148, 2006.

[12] S. F. Cogan, T. D. Plante, and J. Ehrlich, "Sputtered iridium oxide films (SIROF) for low-impedance neural stimulation and recording electrodes," *Proc. 26th Int. Conf. IEEE/EMBS*, 2004, pp. 4153-4156.

[13] J. A. Thornton, "Influence of Apparatus Geometry and Deposition Conditions on Structure and Topography of Thick Sputtered Coatings," *Journal of Vacuum Science & Technology*, vol. 11, pp. 666-670, 1974.

[14] J. Lintymer, J. Gavoille, N. Martin, and J. Takadoum, "Glancing angle deposition to modify microstructure and properties of sputter deposited chromium thin films," *Surface and Coatings Technology*, vol. 174-175, pp. 316-323, 2003.

[15] R. Wuhrer and W. Y. Yeung, "Effect of target-substrate working distance on magnetron sputter deposition of nanostructured titanium aluminium nitride coatings," *Scripta Materialia*, vol. 49, pp. 199-205, 2003.

[16] J. A. Thornton, "Influence of Substrate Temperature and Deposition Rate on Structure of Thick Sputtered Cu Coatings," *Journal of Vacuum Science & Technology*, vol. 12, pp. 830-835, 1975.

[17] J. A. Thornton, "The microstructure of sputter-deposited coatings," *Journal of Vacuum Science & Technology A*, vol. 4, pp. 3059-3065, 1986.

[18] S. Senthil Nathan, G. Mohan Rao, and S. Mohan, "Transport of sputtered atoms in facing targets sputtering geometry: A numerical simulation study," *Journal of Applied Physics*, vol. 84, pp. 564-571, 1998.

[19] W. D. Westwood, "Calculation of Deposition Rates in Diode Sputtering Systems," Journal of Vacuum Science & Technology, vol. 15, pp. 1-9, 1978.